JOURNAL OF SOLID STATE CHEMISTRY **126,** 74–79 (1996)
ARTICLE NO. 0312

Structural Stability and Valence Characteristics in Cerium Hydrothermal Systems

Guangshe Li and Shouhua Feng[1]

Key Laboratory of Inorganic Hydrothermal Synthesis, Jilin University, Changchun 130023, People's Republic of China

and

Liping Li

Department of Physics, Jilin University, Changchun 130023, People's Republic of China

Received January 26, 1996; in revised form June 14, 1996; accepted June 18, 1996

Structural stability and valence characteristics in cerium-containing hydrothermal systems were investigated by means of powder X-ray diffraction, infrared, and X-ray photoelectron spectroscopies. Different input species resulted in the stabilization of cerium in different valence states, e.g., direct formation of CeO_2 and a novel phase $CeOHCO_3$, isostructural with $LaOHCO_3$. High-temperature calcination of $CeOHCO_3$ led to the formation of CeO_2 with high crystallinity and dark brown color. In cerium sulfate systems, both CeO_2 and $Ce(OH)_3$ were found, whereas in nitrate system, ceria with high crystallinity existed as the most stable phase. The mechanisms of the hydrothermal crystallization were discussed and compared with the thermal decomposition reactions of cerium-containing systems.

INTRODUCTION

Cerium compounds have been employed as essential compositions in several kinds of important materials such as electronic-type high-temperature superconductor Nd–Ce–Cu–O and solid electrolytes such as $SrCeO_3$ and CeO_2. By doping lanthanide or alkaline earth elements into CeO_2 or chemically varying the valence state of cerium, mixed conductors may be obtained. However, either electronic conductivity or ionic transport property has been closely related to the valence state and defect property (1). In general, cerium ions in solid compounds exist in 4+ valence, but under certain conditions, the structural stability may alter, for example, the structure of ceria may transform from CaF_2 to $PbCl_2$ type by high pressure (2, 3). Atmosphere treatments on ceria, by changing the stoichiometry (i.e., inducing the oxygen vacancies) and valence state (4), may also change the transport properties.

[1] To whom correspondence should be addressed.

It has been noted that different synthetic routes or treatments may have predominant effects on structural stabilities and properties of as-made products. Thermolysis of cerium inorganic salts, as a most effective method, has been extensively applied to preparing simple cerium oxides, mainly owing to its simple experimental procedure and the variety of products with different structures, valence states, and thermodynamic properties (5, 6). Hydrothermal synthesis which contributes to the preparation of microporous crystals (7, 8), ionic conductors (9–11), layered compounds (12–14), perovskite oxides, etc., unites the features of both high temperature–pressure and soft chemistry, and it has several interesting characteristics in the preparation of cerium compositions. First, the choice of the input species affects the structural stabilities of the final products as Sawyer *et al.* (15) indicated that $LaOHCO_3$ can be obtained from the La_2O_3–H_2O system; however, $La(OH)_3$ was most stable in the $La(NO_3)_3$–$NaOH$–H_2O system. Second, hydrothermal synthesis may lead to valence variations. Nobukazu and Nobuhiro (16) observed mixed valence of bismuth in hydrothermally preparing bismuth oxides. Third, hydrothermal synthesis helps to prepare materials associated with special properties. Le Loarer *et al.* (17, 18) produced ceria with high surface area by treating, at different temperatures, cerium hydroxide obtained at the temperature and pressure below the critical point of the media. Therefore, by varying experimental factors such as input species, pH, crystallization temperature, etc., one can hydrothermally prepare compounds with special compositions and structures which cannot be obtained by conventional preparative methods.

In the present paper, we investigate the direct hydrothermal synthesis of CeO_2, $Ce(OH)_3$, and $CeOHCO_3$ and the relationships among the input species, the structural

0022-4596/96 $18.00

stability of cerium compositions, and the valence state of cerium in hydrothermal systems.

EXPERIMENTAL

The chemicals $Ce_2(C_2O_4)_3 \cdot 10H_2O$ (A.R.), $2(NH_4)_2SO_4 \cdot Ce(SO_4)_2 \cdot 4H_2O$ (A.R.), $Ce_2(SO_4)_3 \cdot 8H_2O$ (Merck), $Ce(SO_4)_2 \cdot 4H_2O$ (A.R.), and $Ce(NO_3)_3 \cdot 6H_2O$ (A.R.) were used as the starting materials in syntheses. NaOH served as a mineralizer. The typical synthetic procedure is described as follows. The reaction reagent selected was first dissolved into the deionized water to form a solution (except cerium oxalate due to its low solubility in water), to which NaOH solution was added dropwise with magnetic stirring to adjust pH of the solution. In some cases, light yellowish colored suspension can be obtained. The initial mole ratios of the input species were kept in the range 2.5–3.5 NaOH : 1.45–2.76 CeO_2 : 600 H_2O. The reaction mixtures were then sealed into 14-ml Teflon-lined stainless steel autoclaves and crystallized at 240°C for 2–3 days. After the autoclaves were cooled and depressurized, the final powder products were washed with deionized water until pH = 7 and dried in air at ambient temperature.

The phases in all powder products were identified by means of X-ray diffraction (XRD) on a Rigaku, D/max-γA, 12-kW XRD diffractometer with a rotating target and Ni-filtered Cu$K\alpha$ radiation at room temperature. Silicon powder (99.99% purity) was used as the external standard for accurate peak position determination. The lattice parameters of the samples were refined by least-squares methods.

The valence state of cerium in the samples was determined by X-ray photoelectron spectroscopy (XPS). The XPS for powder samples fixed on double-sided tapes was measured on an ESCA-LAB MKII X-ray photoelectron spectrometer from the VG Co. with Al$K\alpha$ radiation, and the base pressure was 10^{-7} Pa. C_{1s} signal was used to correct the charge effects.

The infrared (IR) spectra for pressed pellet samples obtained by mixing KBr powder were recorded on a Nicolet 5DX IR spectrometer.

RESULTS AND DISCUSSION

1. Cerium Oxalate Hydrothermal System

In the hydrothermal synthesis, pH and input species were the most important factors affecting the formation of final products, while the latter also determined the sorts and purity of the final products. Selected experimental conditions and results by using different cerium salts as input species are listed in Table 1. It is helpful to make a comparison between thermolysis and hydrothermal reaction for understanding the hydrothermal crystallization mechanisms. Thermolysis of ammonium cerium(III) oxalate hydrate always produces several intermediate phase products such as $Ce_2(C_2O_4)(CO_3)_2$, $Ce_2(CO_3)_3$, and $Ce_2O(CO_3)_2$ (5), while by decomposing lanthanide (except lanthanum) oxalate salts, one can obtain rare earth hydroxide carbonate and carbonates with low stability. The preparation of simple oxides with the least amount of carbonates needed firing temperature above 800°C, whereas lower firing temperature in a range of 300–400°C was often needed in preparing ceria with high surface area.

In contrast with thermolysis, in the hydrotherml systems with a precursor of cerium oxalate and at a crystallization temperature as low as 240°C (in Table 1), no intermediate phases such as those produced in thermolyses were found but $CeOHCO_3$ existed as the most stable phase. It was noted that with a little more complex procedure Haschke (19) prepared the orthorhombic $LaOHCO_3$ in the course of investigating the hydrothermal phase equilibrium in the lanthanum–hydroxide–fluoride–carbonate system. The XRD data for $CeOHCO_3$ are listed in Table 2. The structure of the novel $CeOHCO_3$, an analog of $LaOHCO_3$, was indexed in hexagonal symmetry with cell parameters a = 1.253(3) nm, c = 1.000(2) nm, α = 120°, v = 1.359(1) nm^3 and c/a = 0.798(4). IR spectra were recorded and compared with those of other ceria samples, as shown in Fig. 1, and a very strong absorption at ~3500 cm^{-1} of the OH^- vibration and that at ~1200 cm^{-1} of carbonate ionic species were observed, clearly indicating the existence of OH^- and CO_3^{2-} ions.

It was interesting to find that when $CeOHCO_3$ was calcinated in air at 700, 900, and 1000°C for 0.5, 1, and 2.5 h, respectively, a darker brown CeO_2 was formed, which was different from the commercial yellowish CeO_2, though they all have the same structure as CaF_2, justified by their similar powder XRD patterns. As the calcination temperature increases, the crystallinity and grain size of the CeO_2 powder increase. The reason for darker brown CeO_2 after calcination may be due to the presence of some trivalent cerium in $Ce^{4+}_{1-x}Ce^{3+}_xO_{2-x/2}$, different bond length, and vibration frequencies, which have been confirmed by its particular photovoltage spectrum.

In order to determine the valence state of cerium, the surface XPS of $CeOHCO_3$, the CeO_2 obtained by calcinating $CeOHCO_3$ at 1000°C, and the ceria obtained directly from the nitrate system were measured. The core level spectra are shown in Fig. 2, and binding energies are given in Table 3. Many studies on XPS spectra of Ce(III) and Ce(IV) had shown that, in Ce3d spectra, the characteristic peak at the higher binding energy of 916 eV corresponds to Ce(IV) (20), and in the trace of trivalent cerium, the peak shift of the Ce3$d_{5/2}$ may be used to determine the existence of Ce(III) in the sample (21). From Fig. 2, it can be seen that the binding energy at the main peak of Ce3$d_{5/2}$ of $CeOHCO_3$ is 885.65 eV, the same value as that of standard Ce(III) sample $Na_3Ce(PO_4)_2$. However, another

TABLE 1
Selected Experimental Conditions and Results of the Cerium Compounds in Hydrothermal Systems

Input species	Mineralizer	Reaction temperature (°C)	Reaction time (days)	XRD results	Color of the final products
$Ce_2(C_2O_4)_3$	NaOH	240	2–3	$CeOHCO_3$	Light gray
$2(NH_4)SO_4$	NaOH	240	3	CeO_2	Light yellowish
$\cdot Ce(SO_4)_2$	NaOH	240	3	CeO_2	Light yellowish
$Ce_2(SO_4)_3$	NaOH	240	3	$Ce(OH)_3$	Light yellowish
$Ce(NO_3)_3$	NaOH	240	3	CeO_2	Light gray

peak of 916 eV appeared at the higher binding energy in the Ce3*d* spectra, which shows a small amount of Ce^{4+} existing in the sample measured. Combining the analysis of XRD, it can be concluded that these Ce^{4+} ions come from the trace of CeO_2. Ce3*d* spectra of the ceria after calcinating $CeOHCO_3$ at 1000°C change obviously, the main peak position of $3d_{5/2}$ shifts to 882.2 eV, and the intensity of the peak near 916 eV enhances markedly, which further proves that, after calcination, cerium ions turn into 4+ valence completely. However, it was surprising that all the peaks of ceria after calcination shift 0.6 eV to lower binding energy, in comparison with those in ceria obtained directly from the nitrate hydrothermal system.

TABLE 2
XRD data for $CeOHCO_3$ Obtained in a Cerium Oxalate Hydrothermal System

h	*k*	*l*	d_{cal}	d_{obs}	I/I_o
0	0	2	4.999	5.000	100
2	1	0	4.102	4.107	3
1	1	2	3.908	3.914	3
3	0	0	3.617	3.619	79
0	3	2	2.931	2.932	79
2	2	2	2.655	2.655	3
0	0	4	2.499	2.500	20
4	1	1	2.304	2.305	4
4	1	2	2.140	2.139	3
3	3	0	2.085	2.089	27
3	0	4	2.056	2.056	51
3	3	2	1.927	1.928	27
6	0	0	1.809	1.810	11
6	0	2	1.701	1.702	17
0	0	6	1.666	1.667	6
3	3	4	1.603	1.603	15
3	0	6	1.513	1.514	14
0	6	4	1.465	1.466	9
6	3	0	1.367	1.368	8
6	3	2	1.319	1.319	12
3	3	6	1.303	1.300	3
5	5	0	1.253	1.250	2
6	0	6	1.225	1.226	4
6	4	2	1.208	1.206	3

The peak of O1*s* of the sample $CeOHCO_3$ is at 531.35 eV, which is different from those of O1*s* in normal cerium-containing oxides; it may be contributed by OH^- and CO_3^{2-}. The asymmetry of the spectra at the low binding energy shows the existence of other species of oxygen. From the analyses of Ce3*d* and XRD, it can be concluded that the peak at low binding energy is induced by the trace of ceria. The difference of binding energy of O1*s* in ceria obtained by these two methods is 0.6 eV. The binding energy differences (ΔBE) between $Ce3d_{5/2}$ and O1*s* are given in Table 3. It can be seen that the ΔBE of these two ceria are the same, which indicates that, in these two ceria, there is no change of covalence of the Ce–O bond. The shift of binding energy may be due to the change in Fermi level induced by the alternation of electronic states. It may be the alternation of electronic states that results in the brown color in the calcinated samples.

2. Cerium Sulfate and Nitrate Hydrothermal Systems

It was mentioned above that thermolysis of the hydrate cerium sulfate salts produced some intermediate phases (such as $Ce_2(SO_4)_3$ at ~200°C and $Ce_2O_2SO_4$ above 800°C) ahead of the formation of single-phase ceria. Pokol *et al.* (22) found changes in the oxidation state of cerium in the decomposition of ammonium sulfate complexes of cerium(IV). Chouaib *et al.* (23) indicated that $Ce(OH)_3$ was stable in the whole composition range of concentrated H_2O–NaOH mixtures and found nonstoichiometric cerium oxides in such mixtures as hydrate cerium(III) nitrate and cerium (IV) sulfate precursors. But in their experiments, no $CeOHCO_3$ was formed, and because no hydrothermal crystallization was carried out, only amorphous cerium oxide or a less crystallized product was obtained.

Three cerium sulfate salts and one nitrate salt were used as the input species in the hydrothermal systems. Here again we found that different input species led to different products, although other experimental conditions were kept the same. In the ammonium ceric sulfate and ceric sulfate systems, CeO_2 formed as the most stable phase, while in cerium sulfate, $Ce(OH)_3$ appeared. From the half-width of the diffraction peaks of XRD, it was estimated

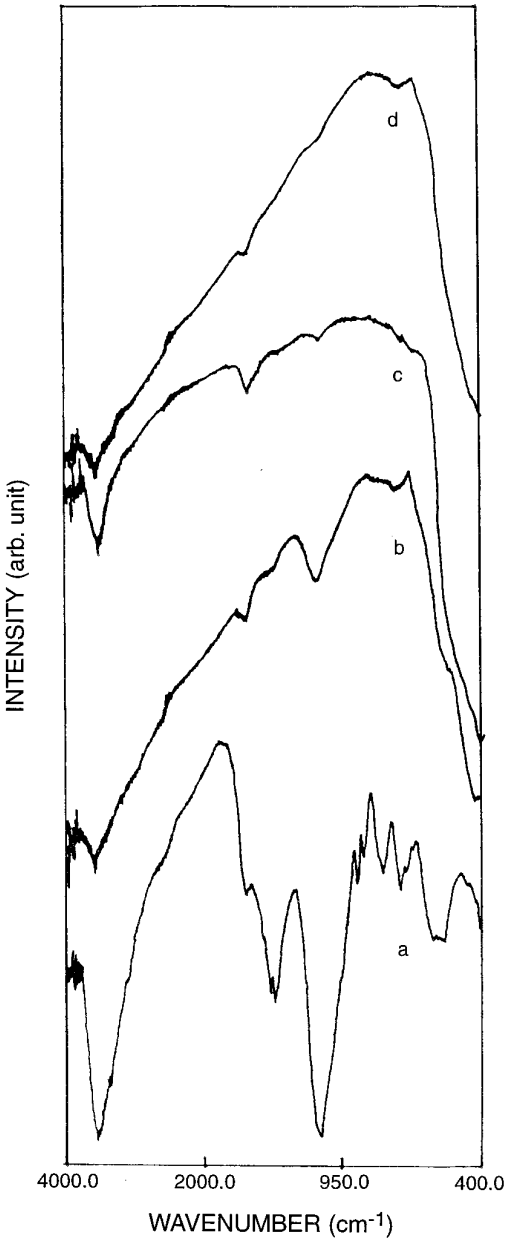

FIG. 1. IR spectra for the samples (a) $CeOHCO_3$, (b) ceria obtained by calcinating $CeOHCO_3$ at 1000°C in air, (c) ceria obtained directly from a cerium nitrate hydrothermal system, and (d) commercial ceria.

that, in the cerium sulfate system, with a small variation of the experimental conditions, both coarse and fine grain ceria can be obtained, whereas in ammonium ceric sulfate system only coarse ceria was formed. In the hydrothermal systems, both CeO_2 and $Ce(OH)_3$ could be directly obtained as pure phases in one step.

Though cerium in its salts exhibits a trivalent state in many cases, different treatments often give products of different valence and stability. A typical example is given for cerium nitrate. In a stronger alkali hydrothermal system, most stable CeO_2 with yellowish color and high crystallinity appeared; subsequent calcination in air at high temperatures above 700°C did not change its color and structure, while thermolysis of this cerium nitrate usually resulted in formation of an essential intermediate phase, $CeONO_3$. So, rich structural stabilities and valence anomalies can be expected in cerium-containing products involved in various reaction systems.

Hydrothermal reaction models can be proposed based on our experimental observations. All hydrothermal reactions may proceed through the following two distinct reaction steps, the first step being the reaction of reactant precursors with OH^- ions,

$$Ce(SO_4)_2 + 4OH^- = CeO_2(s) + 2SO_4^{2-} + 2H_2O \quad [1]$$

$$2(NH_4)_2SO_4 \cdot Ce(SO_4)_2 + 4OH^- = CeO_2(s) + 4SO_4^{2-} + 4NH_4^+ \quad [2]$$

$$Ce_2(SO_4)_3 + 6OH^- = 2Ce(OH)_3 + 3SO_4^{2-} \quad [3]$$

$$2Ce(NO_3)_3 + 6OH^- + 1/2O_2(g) = 2CeO_2(s) + 6NO_3^- + 3H_2O \quad [4]$$

$$Ce_2(C_2O_4)_3 + 8OH^- + 3/2O_2(g) = 2CeOHCO_3 + 4CO_3^{2-} + 3H_2O, \quad [5]$$

where $O_2(g)$ is from air. Reactions 1, 3, and 4 were similar to those reported in the literature (23). All resulting cerium-containing products in reactions 1–5 may be amorphous; i.e., the observed light yellowish suspensions in the experimental procedure formed while NaOH was added to the reaction mixtures. Simultaneously, in the cerium nitrate and oxalate systems, valence variation of cerium was found, but no oxidation state change occurred in the cerium sulfate system.

The second step is the hydrothermal crystallization of these amorphous solids. Porous ceria or ceria with high surface area used to be prepared by calcinating these amorphous solids in air at 300–400°C. However, in our work, after hydrothermal crystallization at a lower temperature of 240°C, different products with high crystallinity such as CeO_2, $Ce(OH)_3$, and $CeOHCO_3$ were formed by using different precursors. The most important is the appearance of cerium in different valence states in the cerium oxalate system, which is due to the formation of the trace of ceria and can be explained by the possible reaction

$$2CeOHCO_3 + 4OH^- + 1/2O_2 = 2CeO_2(\text{crystal}) + 3H_2O + 2CO_3^{2-}. \quad [6]$$

The reaction of the small amount of oxygen inside the

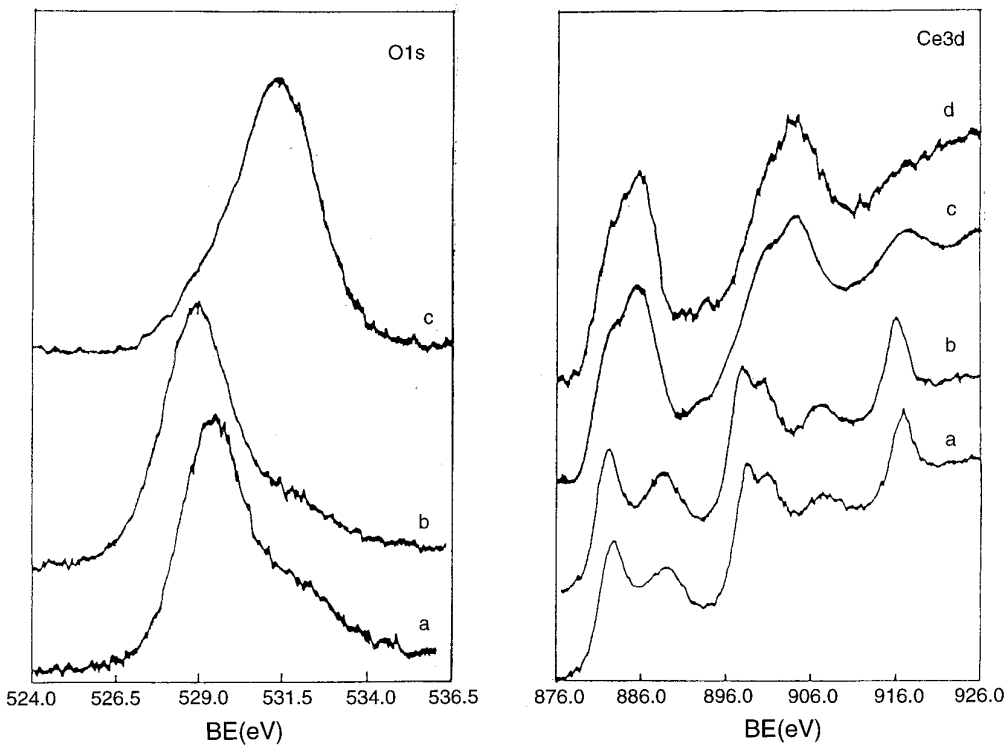

FIG. 2. X-ray photoelectron spectra of the O1*s* and Ce3*d* levels for ceria obtained directly from cerium nitrate hydrothermal system (a), ceria obtained by calcinating $CeOHCO_3$ at 1000°C (b), $CeOHCO_3$ (c), and $Na_3Ce(PO_4)_2$ for comparison.

alkali hydrotherml system with part of $CeOHCO_3$ accounts for the formation of crystalline ceria and valence variation. Thus, the choice of precursors determines, through different reaction models, the structural stability and valence state of cerium in the final products. The above reactions involving OH^- species also indicate that the stronger alkali condition is needed for the hydrothermal crystallization.

CONCLUSIONS

In this work, crystalline CeO_2 was synthesized directly from hydrothermal systems. Different input species resulted in different structural stabilities and valence states of cerium in the cerium compounds in hydrothermal systems. In oxalate systems, a novel hydroxide carbonate, $CeOHCO_3$, was first obtained, in which valence variation was observed. In cerium sulfate systems, both ceria and cerium hydroxide were found, whereas in nitrate systems, ceria with high crystallinity formed as the most stable phase. In hydrothermal synthesis, samples such as ceria can be obtained in one step without producing other intermediate phases essential in thermolyses of cerium inorganic salts. The sorts and the valence state of the resulting products can be controlled by using different input species.

TABLE 3
The Binding Energy of XPS Core Level (eV)

Sample	O1*s*	Ce3$d_{5/2}$		ΔBE
CeO_2 (1)[a]	529.5	882.8	889.2	353.3
CeO_2 (2)	528.9	882.2	888.6	353.3
$CeOHCO_3$	531.4	883.1	885.7	354.3

Note. ΔBE is the difference between the binding energies of Ce3d and O1*s*.

[a] CeO_2 (1) corresponds to ceria obtained from cerium nitrate precursor, CeO_2 (2) from $CeOHCO_3$ calcinated at 1000°C for 0.5 h.

ACKNOWLEDGMENTS

The authors thank Professor Q. Wei of the Analysis and Measurement Center, Jilin University for kindly help in XPS measurement and discussion. This work was financially supported by the NSFC through the Hydrothermal Synthesis Chemistry Project of the National Outstanding Youth Science Fund (S.F.).

REFERENCES

1. H. Arashi, H. Naito, and M. Nakata, *Solid State Ionics* **76,** 313 (1995).
2. G. A. Kourouklis, A. Jayaraman, and G. P. Espinasa, *Phys. Rev. B* **37**. 4250 (1988).
3. J. D. Steven , K. V. Yogesh, L. R. Arthur, A. Jayaraman, and G. P. Espinesa, *Phys. Rev. B* **38,** 7755 (1988).

4. C. Padeste, N. W. Cant, and D. L.Trimm, *Catal. Lett*. **24,** 95 (1994).
5. G. A. M. Hussein and H. M. Ismail, *Colloids Surf. A* **95,** 53 (1995).
6. Y. Du, M. Yashima, M. Kalihana, T. Koura, and M. Yoshimara, *J. Am. Ceram. Soc*. **77**, 2783 (1994).
7. R. Xu, J. Chen, and S. Feng (Eds.), ''Chemistry of Microporous Crystals,'' p. 63. Tokyo, 1991.
8. S. Feng, X. Xu, G. Yang, R. Xu, and F. Glasser, *J. Chem. Soc. Dolton Trans*. **13,** 2147 (1995).
9. S. Feng, M. Tsai, and M. Greenblatt, *Chem. Mater*. **4,** 388 (1992).
10. S. Feng and M. Greenblatt, *Chem. Mater*. **4,** 462 (1992).
11. S. Feng, M. Tsai, S. Szu, and M. Greenblatt, *Chem. Mater*. **4,** 468 (1992).
12. Y. An, S. Feng, Y. Xu, R. Xu, and Y. Yue, *J. Mater. Chem*. **4,** 985 (1994).
13. Y. An, S. Feng, Y. Xu, and Y. Yue, *J. Mater. Chem*. **5,** 773 (1995).
14. Y. An, S. Feng, Y. Xu, R. Xu, and Y. Yue, *J. Mater. Res*. **9,** 2745 (1994).
15. J. Sawyer, P. Carlo, and L. Eyring, *Rev. Chim. Miner*. **10,** 93 (1973).
16. K. Nobukazu and K. Nobuhiro, *Mater. Res. Bull*. **30,** 129 (1995).
17. L. Loarer, J. Luc, P. Francoise, and D. Claire, *Fr. Demande Fr* 2,640,954 1990.
18. L. Loarer, J. Luc, P. Francoise, and D. Claire, *Eur. Pat. Appl. Ep* 376,789 1990.
19. J. M. Haschke, *J. Solid State Chem.* **12,** 115 (1975).
20. G. Pralime, B. E. Koel, R. L. Hance, H. L. Lee, and J. M. White, *J. Electron Spectrosc. Relat. Phenom*. **21,** 17 (1980).
21. L. Li, Q. Wei, H. Liu, and W. Shu, *Z. Phys. B* **96,** 451 (1995).
22. G. Pokol, T. Leskelac, and L. Niinistoe, *J. Therm. Anal*. **42,** 343 (1994).
23. F. Chouaib, G. Delgado, P. Beaunier, and G. Picard, *J. Alloy Compd*. **185,** 279 (1992).